Tight-binding lattices with an oscillating imaginary gauge field

Stefano Longhi[*]

Dipartimento di Fisica, Politecnico di Milano and Istituto di Fotonica e Nanotecnologie del Consiglio Nazionale delle Ricerche,
Piazza L. da Vinci 32, I-20133 Milano, Italy

We consider non-Hermitian dynamics of a quantum particle hopping on a one-dimensional tight-binding lattice made of N sites with asymmetric hopping rates induced by a time-periodic oscillating imaginary gauge field. A deeply different behavior is found depending on the lattice topology. While in a linear chain (open boundary conditions) an oscillating field can lead to a complex quasienergy spectrum via a multiple parametric resonance; in a ring topology (Born–von Karman periodic boundary conditions) an entirely real quasienergy spectrum can be found and the dynamics is pseudo-Hermitian. In the large-N limit, parametric instability and pseudo-Hermitian dynamics in the two different lattice topologies are physically explained on the basis of a simple picture of wave-packet propagation.

I. INTRODUCTION

Non-Hermitian models have attracted since many years a considerable attention in different areas of physics with applications in a variety of fields, including the quantum mechanics of open systems [1,2], parity-time ($\mathcal{PT}$) symmetric quantum mechanics and quantum field theories [3], atom optics [4], hydrodynamics [5], superconductors [6], biological [7], and optical [8–10] systems to mention a few.

Among the various non-Hermitian quantum models, great attention has been devoted to the study of the hopping dynamics of a quantum particle in a lattice in the presence of an "imaginary" vectorial potential. Such a model was introduced in 1996 by Hatano and Nelson [6] in the context of flux lines in superconductors. They investigated the problem of Anderson localization in a disordered non-Hermitian lattice and showed that an imaginary magnetic field can prevent Anderson localization, with the appearance of a mobility interval at the center of the band (non-Hermitian delocalization transition). Such a result was subsequently revisited by several authors [11] and connected to the problem of the spectrum of tridiagonal random matrices and random Dirac fermion models [12]. While the realization of a synthetic imaginary magnetic field in the solid-state context is challenging, in optics a rather simple implementation of the Hatano–Nelson model with an artificial imaginary gauge field has been recently proposed [13,14]. This model is based on light transport in a chain of coupled optical microrings with tailored gain and loss regions. Such a photonic analog of the Hatano–Nelson model is expected to provide a viable route toward an experimental observation of non-Hermitian delocalization transition and non-Hermitian transparency.

In such previous studies [6,11–15] the imaginary gauge field was considered stationary. However, it is well known that, in ordinary tight-binding Hermitian quantum models, oscillating electric and/or magnetic fields can deeply change the hopping dynamics via a Peierls' substitution with important applications to coherent quantum-state storage, dynamic decoupling, and decoherence control (see, for instance, Ref. [16]

and references therein). In one-dimensional lattices, oscillating fields renormalize the effective hopping rates and can result in coherent destruction of tunneling and dynamic localization [17,18], which have been observed in matter wave and optical systems [19,20]. In two-dimensional lattices, gauge fields are responsible for many important phenomena related to quantum Hall physics, topological insulators, and new phases of matter [21]. Recent works have investigated the properties of time-periodic $\mathcal{PT}$ symmetric Hamiltonians, highlighting some interesting physical effects that arise from the interplay between non-Hermitian dynamics and periodic driving [22–27]. In particular, non-Hermitian extensions of the Rabi model have been introduced, i.e., a two-level system driven by an *imaginary* field, revealing some interesting physics such as the non-Hermitian analog of the Bloch–Siegert shift, $\mathcal{PT}$-symmetry breaking and restoration via higher-order parametric resonances, and the possibility to simulate Hofstadter's butterfly spectrum for a class of superlattice Hamiltonians [25–27].

Motivated by such previous works, we introduce in this paper a time-periodic extension of the non-Hermitian Hatano–Nelson Hamiltonian that describes the quantum dynamics of a particle hopping on a tight-binding lattice with an *oscillating* imaginary gauge field. Likewise, for static $\mathcal{PT}$ lattices that show different phase diagrams for ring and line topologies [28–30], we find two distinct dynamical regimes; namely, oscillation-induced pseudo-Hermitian dynamics in the ring topology and multiparametric instability in the line topology. For a quantum particle hopping on a ring threaded by an imaginary gauge flux, the energy spectrum in a stationary gauge field is always complex; however, the addition of an ac (oscillating) gauge field can result in an entirely real quasienergy spectrum, i.e., the oscillating field can lead to a stabilization effect and pseudo-Hermitian dynamics (Sec. II). A fully different scenario is found for a particle hopping on a finite linear chain with open boundary conditions (Sec. III). In this case the energy spectrum is entirely real for a stationary imaginary gauge field since the non-Hermitian problem with open boundary conditions is pseudo-Hermitian and can be mapped onto an equivalent Hermitian model via an imaginary gauge transformation. However, application of an oscillating imaginary gauge field breaks pseudo-Hermiticity and the
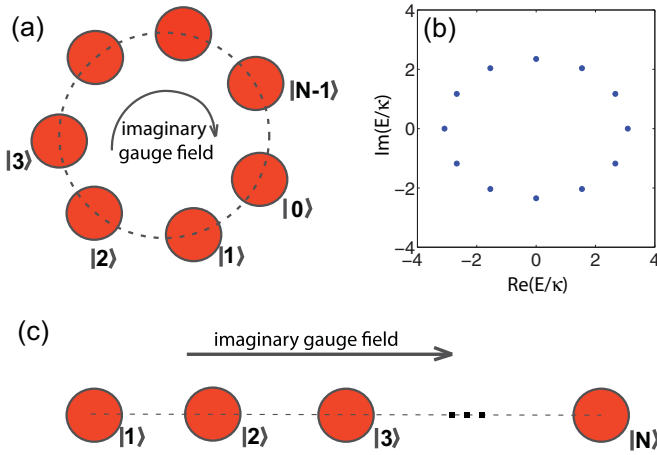
————
[*]stefano.longhi@polimi.it

FIG. 1. (a) Schematic of a tight-binding ring threaded by an imaginary gauge field $h = h(t)$. (b) Energy spectrum of the Hamiltonian (1) for a ring comprising $N = 12$ sites in a stationary gauge field $h = h_0 = 1$. The energies in the complex plane lie on the ellipse defined by Eq. (7). (c) Schematic of a linear chain, comprising N lattice sites with an imaginary and time-dependent gauge field. Left and right hopping rates are $\kappa \exp[h(t)]$ and $\kappa \exp[-h(t)]$, respectively.

quasienergy spectrum can become complex via multiple parametric resonances. A simple physical explanation of the different dynamical scenario found in the two tight-binding lattices with different topology is also presented (Sec. IV).

II. PSEUDO-HERMITIAN DYNAMICS IN A TIGHT-BINDING RING THREADED BY AN OSCILLATING IMAGINARY GAUGE FIELD

Let us consider the hopping motion of a quantum particle on a tight-binding ring comprising $N \geqslant 3$ sites threaded by an imaginary and time-dependent gauge field $h = h(t)$; see Fig. 1(a). The non-Hermitian tight-binding Hamiltonian of the ring reads

$$\hat{H}(t) = \kappa \sum_{n=0}^{N-1} [\exp(h)|n\rangle\langle n+1| + \exp(-h)|n+1\rangle\langle n|], \quad (1)$$

where κ is the hopping rate, $h = h(t)$ is the imaginary gauge field, and the periodic (Born–von Karman) boundary condition $|n + N\rangle = |n\rangle$ applies. After setting $|\psi(t)\rangle = \sum_{n=0}^{N-1} c_n(t)|n\rangle$, from the Schrödinger equation $i\partial_t|\psi(t)\rangle = \hat{H}(t)|\psi(t)\rangle$, the following coupled differential equations for the site amplitude probabilities $c_n(t)$ are found:

$$i\frac{dc_n}{dt} = \kappa \exp[h(t)]c_{n+1} + \kappa \exp[-h(t)]c_{n-1} \quad (2)$$

$(n = 0, 1, 2, \ldots, N-1)$, with the periodic boundary conditions $c_n(t) = c_{n+N}(t)$. Let us first recall the properties of the energy spectrum of $\hat{H}$ in the stationary case $h = h_0$ constant, which were discussed in previous works [6,11]. The eigenfunctions and corresponding energies of $\hat{H}$ are given by $c_n^{(l)}(t) \propto \exp(iq_l n - iE_l t)$ and $E_l = 2\kappa \cosh(h_0)\cos(q_l) + 2i\kappa \sinh(h_0)\sin(q_l)$, respectively, where $q_l = 2\pi l/N$ is the quantized Bloch wave number $(l = 0, 1, 2, \ldots, N-1)$. Note that the energy spectrum is complex and the eigenvalues E_l lie

on the ellipse

$$\left[\frac{\text{Re}(E)}{\cosh(h_0)}\right]^2 + \left[\frac{\text{Im}(E)}{\sinh(h_0)}\right]^2 = 4\kappa^2, \quad (3)$$

as already shown in previous works [6,11]. An example of the energy spectrum is shown in Fig. 1(b).

The most general solution to Eq. (2) with $h(t) = h_0$ constant is given by $c_n(t) = \sum_{m=0}^{N-1} \mathcal{U}_{n,m}^0(h_0; t)c_m(0)$ with the propagator $\mathcal{U}_{n,m}^0(h_0; t)$

$$\mathcal{U}_{n,m}^0(h_0; t) \equiv \frac{1}{N} \sum_{\sigma=0}^{N-1} \exp[iq_\sigma(n-m) - iE_\sigma t]. \quad (4)$$

Note that, in the Hermitian limit $h_0 = 0$, the ellipse defined by Eq. (3) shrinks into a line on the real axis (real energy spectrum) and the propagator $\mathcal{U}_{n,m}^0$ defined by Eq. (4) with $h_0 = 0$ is unitary and describes a quasiperiodic dynamics on the ring.

Let us now consider the more general case of a time-dependent imaginary gauge field $h = h(t)$. The most general solution to Eq. (2) is given by $c_n(t) = \sum_{m=0}^{N-1} \mathcal{U}_{n,m}(t)c_m(0)$, where the propagator $\mathcal{U}_{n,m}(t)$ can be formally written as the ordered product

$$\mathcal{U}(t) = \lim_{S \to \infty} \prod_{k=1}^{S} \mathcal{U}^0(h_k; \Delta t)$$

$$= \lim_{S \to \infty} \mathcal{U}^0(h_S; \Delta t)\mathcal{U}^0(h_{S-1}; \Delta t) \cdots \mathcal{U}^0(h_1; \Delta t). \quad (5)$$

In the previous equation, $\Delta t = t/S$, $t_k = k\Delta t$, and $\mathcal{U}^0(h; \Delta t)$ is defined by Eq. (4). After some simple algebra one obtains

$$\mathcal{U}_{n,m}(t) = \frac{1}{N} \sum_{\sigma=0}^{N-1} \exp\left[iq_\sigma(n-m) - i\int_0^t dt' E_\sigma(t')\right], \quad (6)$$

where $E_\sigma(t)$ is defined by

$$E_\sigma(t) = 2\kappa \cos(q_\sigma)\cosh[h(t)] + 2i\kappa \sin(q_\sigma)\sinh[h(t)]. \quad (7)$$

Note that the propagator $\mathcal{U}(t)$ in the time-dependent case [Eq. (6)] is a simple extension of the propagator $\mathcal{U}^0(t)$ in the time-independent case [Eq. (4)] via the substitution $E_\sigma t \to \int_0^t dt' E_\sigma(t')$. Such a property mainly stems from the fact that the eigenfunctions of $\hat{H}$ with $h(t) = h_0$ constant are independent of h_0. Let us specialize our general result to the case of a time-periodic gauge field $h(t)$ with frequency ω and period $T = 2\pi/\omega$, i.e., $h(t + T) = h(t)$. In this case, from Eq. (6) it readily follows that the N quasienergies E_l of the time-periodic Hamiltonian $\hat{H}(t)$ are given by

$$E_l = 2\kappa \cos q_l \left(\frac{1}{T}\int_0^T dt \cosh[h(t)]\right)$$

$$+ 2i\kappa \sin q_l \left(\frac{1}{T}\int_0^T dt \sinh[h(t)]\right). \quad (8)$$

As in the time-independent case, the quasienergies are complex and lie on the ellipse of the equation

$$\left[\frac{\mathrm{Re}(E)}{\frac{1}{T}\int_0^T dt\,\cosh h(t)}\right]^2 + \left[\frac{\mathrm{Im}(E)}{\frac{1}{T}\int_0^T dt\,\sinh h(t)}\right]^2 = 4\kappa^2. \quad (9)$$

Interestingly, whenever the condition

$$\int_0^T dt\,\sinh[h(t)] = 0 \quad (10)$$

is satisfied, the quasienergy spectrum becomes real, and at the stroboscopic propagation times $t = T, 2T, 3T, \ldots$ the time-periodic non-Hermitian Hamiltonian $\hat{H}(t)$ is equivalent to the effective stationary and Hermitian Hamiltonian of a tight-binding ring

$$\hat{H}_{\mathrm{eff}} = \kappa_{\mathrm{eff}} \sum_{n=0}^{N-1} (|n\rangle\langle n+1| + |n+1\rangle\langle n|) \quad (11)$$

with enhanced hopping rate

$$\kappa_{\mathrm{eff}} = \kappa\left(\frac{1}{T}\int_0^T dt\,\cosh[h(t)]\right). \quad (12)$$

Therefore, provided that the condition (10) is met, the quantum dynamics of a particle on a ring described by the time-periodic non-Hermitian Hamiltonian (1) is pseudo-Hermitian and the role of the oscillating field is to stabilize the dynamics. Note that the condition (10) is satisfied for any arbitrary ac field $h(t)$ with zero mean satisfying the odd-symmetry constraint $h(-t + t_0) = h(t_0 + t)$ for some t_0; for example, for a sinusoidal field $h(t) = h_1 \sin(\omega t)$ regardless of the amplitude and frequency of the oscillation. Remarkably, the condition (10) can be met even for time-periodic fields $h(t)$ with a nonvanishing dc term, which is a nontrivial result. For example, let us consider the piecewise constant field $h(t)$ defined by

$$h(t) = \begin{cases} h_1, & 0 < t < T_1 \\ -h_2, & T_1 < t < T \end{cases} \quad (13)$$

in the period $(0,T)$, with $h_1, h_2 > 0$. Provided that $h_1 T_1 \neq h_2 T_2$, where $T_2 = T - T_1$, the field $h(t)$ has a non vanishing dc term. Furthermore, if the condition $T_1 \sinh h_1 = T_2 \sinh h_2$ holds, Eq. (10) is met and the dynamics is pseudo-Hermitian. Such a result shows that, *rather generally*, the addition of an ac field to a dc imaginary gauge field can lead to stabilization (real quasienergy spectrum) and pseudo-Hermitian dynamics.

An example of pseudo-Hermitian dynamics on a ring comprising $N = 3$ sites with a sinusoidal imaginary gauge field $h(t) = h_1 \sin(\omega t)$ is shown in Fig. 2 for parameter values $\omega/\kappa = 1$ and $h_1/\kappa = 0.4$. The solid curves in the figure depict the numerically computed evolution of the site occupation amplitudes $|c_n(t)|$ at the three sites $n = 0,1,2$ with the initial condition $c_n(0) = \delta_{n,0}$, corresponding to excitation of site $n = 0$. According to Eqs. (8) and (12), the quasienergies are given by $E_l = 2\kappa_{\mathrm{eff}} \cos(2\pi l/3)$ ($l = 0,1,2$) with $\kappa_{\mathrm{eff}} = \kappa(1/T)\int_0^T dt\,\cosh[h(t)] \simeq 2.081\kappa$, i.e., there are two distinct quasienergies $E_1/\kappa \simeq -1.0405$ and $E_2/\kappa \simeq 2.081$. Since $|E_2 - E_1|$ is incommensurate with the modulation frequency ω, the dynamics turns out to be aperiodic. The dashed curves in the figure show the numerically computed evolution of
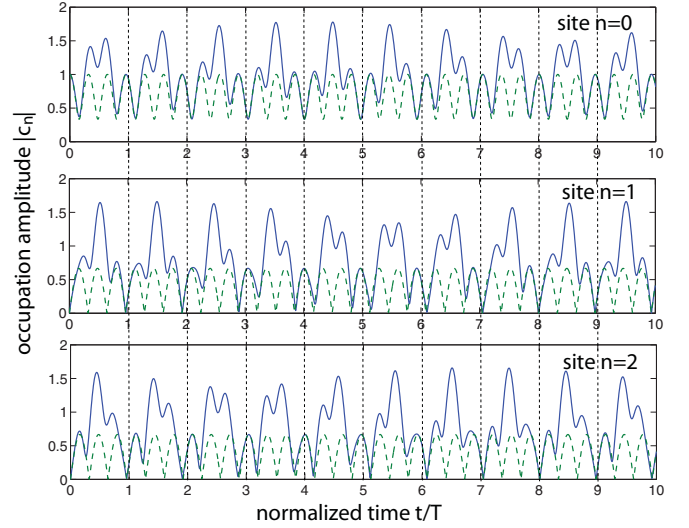

FIG. 2. Pseudo-Hermitian dynamics in a ring, comprising $N = 3$ sites, threaded by an imaginary gauge field $h(t) = h_1 \sin(\omega t)$ for $\omega/\kappa = 1$ and $h_1/\kappa = 0.4$. The solid curves show the evolution of the site occupation amplitudes $|c_n(t)|$ at the three sites for the initial condition $c_n(0) = \delta_{n,0}$. The dashed curves show the corresponding behavior as obtained by using the effective Hermitian Hamiltonian (11). The solid and dashed curves intersect at the discretized times $t/T = 1,2,3,\ldots$ (vertical dotted curves).

the occupation amplitudes at the three sites for the effective stationary Hermitian Hamiltonian (11), which is periodic with period τ given by $\tau/T = \omega/|E_2 - E_1| \simeq 0.32$. Note that, according to the theoretical analysis, at discretized times $t/T = 1,2,3,\ldots$ (vertical dotted curves in Fig. 2) the dynamical behavior of the two Hamiltonians (1) and (11) does coincide.

III. MULTIPLE PARAMETRIC RESONANCE IN A TIGHT-BINDING LINEAR CHAIN WITH AN OSCILLATING IMAGINARY GAUGE FIELD

In the case of static $\mathcal{PT}$-symmetric Hamiltonians, it is known that the phase diagram separating regions of real and complex energies is strongly dependent on the lattice topology, i.e., it differs for ring and line topologies [28–30]. Such a result basically stems from the fact that the $\mathcal{PT}$ symmetry is a nonlocal symmetry. Likewise, we expect that the phase diagram of the tight-binding lattice driven by an oscillating imaginary gauge field is modified when considering a linear chain rather than a ring. In particular, in the linear chain geometry pseudo-Hermitian dynamics is broken owing to the appearance of parametric resonances, which are ubiquitous in the dynamics of time-periodic non-Hermitian Hamiltonians [24–27].

Let us consider the hopping motion of a quantum particle on a linear tight-binding chain comprising $N \geq 2$ sites with an imaginary and time-dependent gauge field $h = h(t)$; Fig. 1(c). The evolution equations for the site amplitude probabilities $c_n(t)$ ($n = 1,2,\ldots,N$) are given by Eq. (2), but now the open boundary conditions $c_0(t) = c_{N+1}(t) = 0$ apply. For a time-independent $h(t) = h_0$ imaginary gauge field, the energy spectrum is entirely real and is given by $E_l = 2\kappa \cos(q_l)$,

where $q_l = l\pi/(N+1)$ ($l = 1,2,\ldots,N$). In fact, after the imaginary gauge transformation $c_n(n) = a_n(t)\exp(-h_0 n)$ the coupled-equations (2) yield

$$i\frac{da_n}{dt} = \kappa a_{n+1} + \kappa a_{n-1}, \qquad (14)$$

which describe the dynamics of a Hermitian tight-binding linear chain with uniform hopping rates. When using the above-mentioned gauge transformation, the most general solution to Eq. (2) with $h(t) = h_0$ and open boundary conditions is given by $c_n(t) = \sum_{l=1}^{N} \mathcal{U}_{n,l}^0(h_0;t)c_l(0)$, with the propagator $\mathcal{U}^0(h_0;t)$ defined by

$$\mathcal{U}_{n,l}^0(h_0;t) = \frac{2}{N+1}\exp[h_0(l-n)]\sum_{\sigma=1}^{N}\sin\left(\frac{\pi n\sigma}{N+1}\right)$$

$$\times \sin\left(\frac{\pi l\sigma}{N+1}\right)\exp\left[-2i\kappa t\cos\left(\frac{\pi\sigma}{N+1}\right)\right]. \tag{15}$$

In the time-dependent case $h = h(t)$, according to Eq. (5) the propagator $\mathcal{U}(t)$ from $t = 0$ to $t = t$ can be formally written as the ordered product of operators $\mathcal{U}^0(h_k;\Delta)$ of the stationary system, where $h_k = h(t_k)$ and $t_k = k\Delta t$. Unlike the ring lattice model considered in the previous section, in this case the product of operators cannot be determined in an analytical form and one has to resort to a numerical analysis. For a time-periodic gauge field with period $T = 2\pi/\omega$, i.e., $h(t + T) = h(t)$, according to Floquet theory the N quasienergies of the time-periodic Hamiltonian $\hat{H}(t)$ are given by $E_l = (i/T)\ln(\mu_1)$, where μ_l ($l = 1,2,\ldots,N$) are the N eigenvalues of the matrix $\mathcal{U}(T)$, i.e., of the propagator over one oscillation period T. A numerical computation of quasienergies for an oscillating field shows rather generally that pseudo Hermitian dynamics can be broken and the quasienergy spectrum can become complex owing to the appearance of resonance tongues, which are the signature of a multiple parametric instability [31–33]. As an example, Fig. 3 shows the numerically computed instability domains (regions of complex quasienergies) in the frequency-amplitude plane (ω, h_1) for a square-wave ac gauge field

$$h(t) = \begin{cases} h_1, & 0 < t < T/2 \\ -h_1, & T/2 < t < T \end{cases} \tag{16}$$

and for a few increasing values of lattice sites N. For a square-wave modulation, the propagator $\mathcal{U}(T)$ over one oscillation cycle is readily computed as $\mathcal{U}(T) = \mathcal{U}^0(-h_1;T/2)\mathcal{U}^0(h_1;T/2)$, where $\mathcal{U}^0$ is defined by Eq. (15). The figure clearly indicates the appearance of resonance tongues emanating from $h_1 = 0$ at certain modulation frequencies ω. The number of resonances increases as the number of site N increases and become densely spaced close to $\omega \to 0$. In the simplest case of two sites ($N = 2$), the instability arises from an ordinary parametric resonance, which for a non-Hermitian $\mathcal{PT}$-symmetric dimer has been studied in Ref. [24]. Similar parametric resonances have been recently found in the study of the non-Hermitian extension of the Rabi model [25–27] comprising two or few states. For a large number of lattice sites in the chain, which is the case of main interest in the present work, instability arises from multiple parametric resonances and the phase diagram
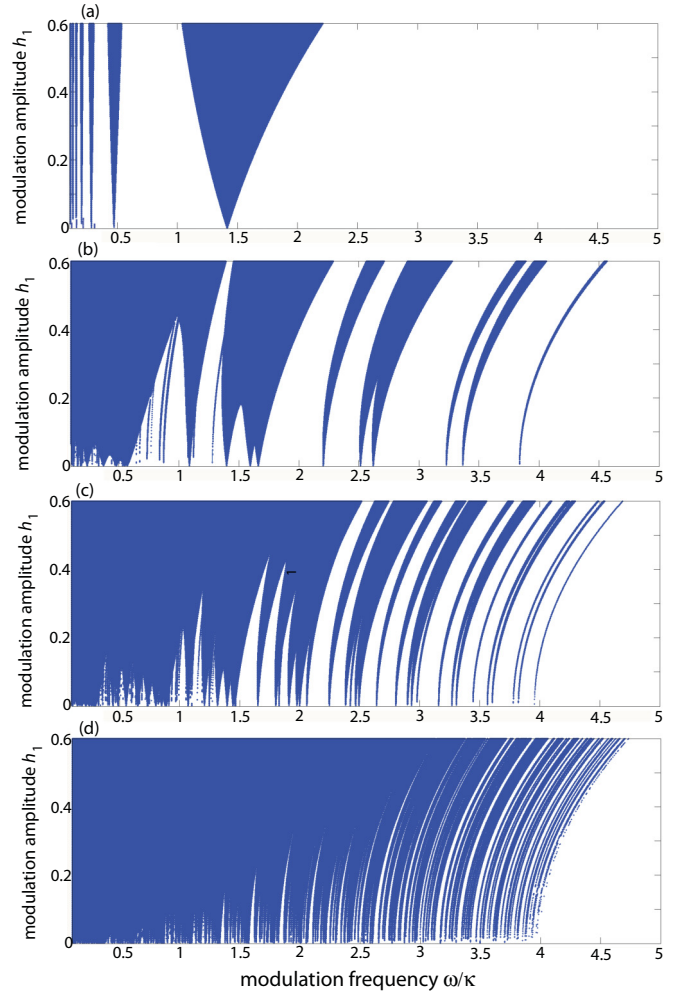

FIG. 3. Numerically computed regions of complex quasienergies (dark areas) arising from multiple parametric resonances for a square-wave modulation $h(t)$ and for an increasing number N of lattice sites: (a) $N = 3$, (b) $N = 10$, (c) $N = 20$, and (d) $N = 50$. The number of resonance tongues rapidly increases, below the cutoff frequency 4κ, as N increases.

shows a dense set of resonance tongues, as shown in Fig. 3. Multiple parametric resonance tongues can be analytically determined by a secular perturbation theory in the $h \to 0$ limit; details are reported in Appendix A. Rather generally, indicating by $l\omega$ the lth harmonic of the modulation function $h(t)$, resonance tongues emanate at the frequencies ω satisfying the condition

$$E_n - E_m \pm l\omega \simeq 0 \tag{17}$$

for some integers $n,m = 1,2,\ldots,N$, where $E_n = 2\kappa\cos[n\pi/(N+1)]$. For symmetry reasons, some such resonances can be missed, as discussed in the appendix for the simple case of $N = 3$ lattice sites [Fig. 3(a)]. As the number N of lattice sites increases, the resonance conditions (17) are satisfied in a dense number of frequencies below the cutoff frequency 4κ, as shown, e.g., in Fig. 3(d) for $N = 50$ sites. Since E_n falls inside the range $(-2\kappa, 2\kappa)$, for a modulation frequency ω larger than 4κ, the resonance condition (17) can never be satisfied. Therefore, for $\omega > 4\kappa$ parametric
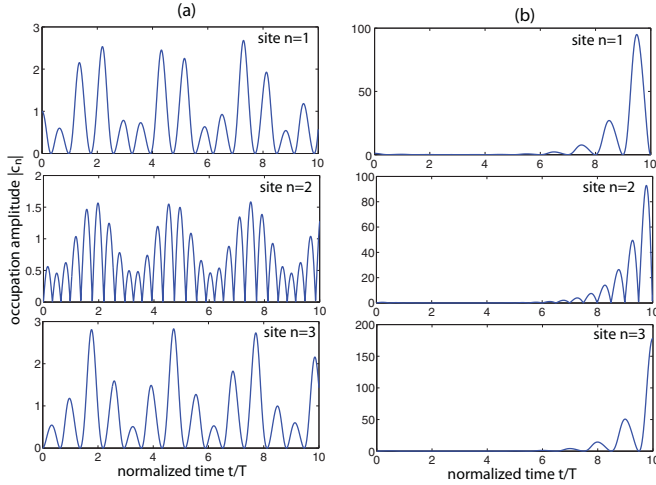
FIG. 4. Parametric instability in a linear chain comprising $N = 3$ sites with an oscillating imaginary gauge field $h(t) = h_1 \sin(\omega t)$ for (a) $\omega/\kappa = 1$, $h_1 = 0.4$, and (b) $\omega/\kappa = \sqrt{2}$, $h_1 = 0.4$. The curves in the various panels show the evolution of the site occupation amplitudes $|c_n(t)|$ at the three sites for the initial condition $c_n(0) = \delta_{n,1}$. In panel (a) the quasienergy spectrum is real and the dynamics is pseudo-Hermitian. In panel (b) the quasienergy spectrum becomes complex owing to parametric resonance, which is clearly manifested in the secular growth of amplitudes $|c_n(t)|$.

resonances are prevented and the quasienergies are entirely real (for a not-too-large value of the modulation amplitude). Such a result is in agreement with the fact that, in the large-modulation-frequency limit, one can average the rapidly oscillating imaginary Peierls' phases in Eq. (2), leading to an effective Hermitian linear chain with hopping rate $(\kappa/T) \int_0^T dt \exp[\pm h(t)]$ (see, for instance, Ref. [22]).

An example of parametric instability on a linear chain comprising $N = 3$ sites with a sinusoidal imaginary gauge field $h(t) = h_1 \sin(\omega t)$ is shown in Fig. 4 for parameter values $\omega/\kappa = 1$ and $h_1 = 0.4$ in Fig. 4(a), and $\omega/\kappa = \sqrt{2}$ and $h_1 = 0.4$ in Fig. 4(b). The curves in the figure depict the numerically computed evolution of the site occupation amplitudes $|c_n(t)|$ at the three sites $n = 1,2,3$ with the initial condition $c_n(0) = \delta_{n,1}$, corresponding to excitation of the edge site $n = 1$. While in Fig. 4(a) the modulation frequency is far from any resonance tongue and the dynamics is pseudo-Hermitian (real quasienergies), in Fig. 4(b) the modulation frequency is set in resonance with the first resonance tongue [see Fig. 3(a)] and an instability is clearly observed, corresponding to a secular growth of amplitudes $|c_n(t)|$ and complex quasienergy spectrum.

IV. PSEUDO-HERMITIAN DYNAMICS AND PARAMETRIC INSTABILITY: A SIMPLE PHYSICAL DESCRIPTION

In the previous two sections we have shown that, when an oscillating imaginary gauge field is applied to a tight-binding lattice, two different phenomena can arise depending on the lattice topology, i.e., on the boundary conditions: pseudo-Hermitian dynamics in a ring lattice, and parametric resonances in a linear chain. While the dependence of the phase diagrams on lattice topology and the onset of parametric resonances are ubiquitous effects of time-periodic
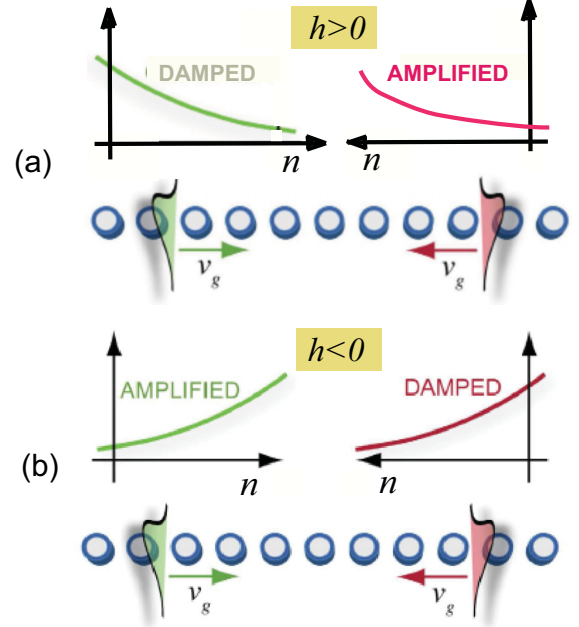

FIG. 5. Schematic of wave-packet propagation in the bulk of a tight-binding lattice with an imaginary gauge field h. For $h > 0$ [panel (a)] a forward-propagating (backward-propagating) wave packet is damped (amplified), whereas for $h < 0$ [panel (b)] the reversed behavior occurs.

non-Hermitian systems [24–30], in the non-Hermitian lattice model with an oscillating imaginary gauge field considered in our work a rather simple and elegant physical explanation of such phenomena can be given by considering the limit of a large number N of lattice sites. In such a limit, the two phenomena can be captured by considering a wave packet that either travels along a ring or propagates back and forth in a linear chain. Let us consider an infinitely extended lattice in the presence of a stationary imaginary gauge field h. As shown in Ref. [13], wave transport in the lattice is highly asymmetric because wave packets propagating in opposite directions are one amplified and the other one damped. Such a property follows from the nature of the dispersion relation of plane waves $c_n(t) \sim \exp[iqn - iE(q)t]$ in the infinitely extended lattice, which reads [13]

$$E(q) = 2\kappa \cosh(h) \cos q + 2i\kappa \sinh(h) \sin q, \quad (18)$$

where $-\pi < q < \pi$ is the Bloch wave number. A wave packet, which is obtained by a superposition of plane waves around a carrier wave number q, propagates with a group velocity $v_g = [d\text{Re}(E)/dq] = -2\kappa \cosh h \sin q$. For $h > 0$, a forward-propagating wave packet $(-\pi < q < 0, v_g > 0)$ is attenuated since $\text{Im}(E) < 0$, whereas a backward-propagating wave packet $(0 < q < \pi, v_g < 0)$ is amplified since $\text{Im}(E) > 0$. The opposite behavior occurs when the sign of the gauge field h is reversed; see Fig. 5.

With such a property in mind, let us first consider propagation of a wave packet in a ring. The ring periodic boundary conditions just introduce a quantization of the wave number q, which, however, for a large number N of sites and a sufficiently localized wave packet does not change the

dynamics as compared with the infinitely extended lattice. Therefore, for a stationary field a localized wave packet is either secularly damped or amplified depending on the circulation direction (either clockwise or counterclockwise). This is in agreement with the fact that, for a time-independent field h, the energy spectrum of the Hamiltonian is complex. However, when the gauge field $h(t)$ oscillates in time, the wave packet undergoes periodic amplification and attenuation, regardless of the circulation direction. In particular, whenever the time-average of the amplification or attenuation rate $\text{Im}(E) = 2\kappa \sin[h(t)] \sin q$ vanishes, secular growth or decay of the wave packet is suppressed, and the dynamics is pseudo-Hermitian. Note that the vanishing, on average, of the amplification or attenuation rate is precisely expressed by the condition (10) derived in Sec. II.

Let us now consider the propagation of a wave packet in a long chain. For a stationary imaginary gauge field h, a forward-propagating wave packet is attenuated. However, when it reaches the right chain boundary, it is reflected, and the backward-propagating wave packet is amplified at the same rate. At the left chain boundary, the wave packet is reflected and the forward-propagating wave packet is damped. Hence a periodic attenuation or amplification occurs in a balanced manner after each reflection at the left or right lattice edges: the dynamics is thus pseudo-Hermitian with no secular growth or attenuation of the wave-packet amplitude on average. When the imaginary gauge field $h(t)$ is an oscillating field with zero mean, $h(t)$ changes sign within each oscillation cycle and the dynamics is strongly dependent on the ratio between the oscillation period and the transit time of the wave packet in the chain. Let us assume for the sake of definiteness that $h(t)$ is positive in the first semicycle of oscillation $0 < t < T/2$ and negative in the second semicycle $T/2 < t < T$. This is the case, for example, of a square wave or of a sinusoidal field. The transit time of the wave packet between the two edges of the chain is $\tau = N/v_g$. If the transit time in an odd multiple, then $T/2$, i.e., for $\tau = (2l + 1)T/2$, an overall amplification in one circulation direction occurs, which cumulates at successive transits back and forth between the two lattice edges. This is because, after each reflection at the lattice edge, the sign of h changes synchronously. As a result, a secular growth of the wave-packet amplitude arises in one circulation direction, which is the signature of the parametric instability. Taking into account that, for $|h(t)| \ll 1$, one has $\tau = N/v_g \simeq N/(2\kappa|\sin q|)$, the condition $\tau = (2l + 1)T/2 = (2l + 1)\pi/\omega$ yields $\omega = 2\kappa\pi(2l + 1)|\sin q|/(N)$. For a long chain, the frequencies at which parametric instability arises are thus a dense set, according to the numerical results [see Fig. 3(d)]. The existence of a cutoff frequency above which parametric instability is suppressed follows from the requirement that the oscillation period T must be longer than the characteristic reflection time τ_R of the wave packet, i.e., $T > \tau_R$. For a wave packet with lattice extension Δn and group velocity v_g, the reflection time can be estimated as $\tau_R \sim \Delta n/v_g$. For a narrow wave packet with lattice extension of a few sites, e.g., taking $\Delta n \sim \pi$, the shortest reflection time is obtained at the carrier Bloch wave number $q = \pi/2$, corresponding to the largest group velocity $v_g \simeq 2\kappa$ and thus to a reflection time $\tau_R \sim \pi/(2\kappa)$. The requirement $T > \tau_R$ thus gives $\omega \lesssim 4\kappa$, which is precisely the cutoff condition rigorously derived in Sec. III.

V. CONCLUSION

Driven tight-binding lattices provide a fertile quantum model for coherent quantum control, dynamic decoupling, and decoherence control in quantum physics [16–18]. The application of oscillating electric or magnetic fields on a particle hopping on a lattice introduces Peierls' phases that can be tailored to realize important effects such as hopping-rate renormalization, coherent destruction of tunneling, dynamic localization, and quantum Hall physics [17–20]. While great attention has been devoted so far to study Peierls' phases in driven Hermitian systems and the related broad fields of artificial gauge fields and novel phases of matter, the effects of an oscillating *imaginary* gauge field have, so far, been overlooked. Imaginary gauge fields were introduced in a pioneering paper by Hatano and Nelson [6] to study non-Hermitian Anderson localization in disordered lattices, which raised a lively interest [11,12]. Recently, the proposal to implement artificial imaginary gauge fields in integrated photonics using coupled optical microrings with tailored gain and loss regions [13,14] has renewed the interest in the Hatano–Nelson model, paving the way toward an experimental demonstration of non-Hermitian Anderson delocalization transition. Such previous studies, however, are limited to consider stationary imaginary gauge fields. In this work we theoretically investigated the quantum dynamics in a one-dimensional tight-binding lattice with an oscillating imaginary gauge field. As compared to the analogous problem of real gauge fields, the imaginary-gauge-field problem discloses a completely different dynamical behavior, which is strongly sensitive to lattice topology even in the one-dimensional case. For a quantum particle hopping on a ring threaded by an imaginary gauge flux, the energy spectrum in a stationary gauge field is always complex; however, the addition of an ac (oscillating) gauge field can result in an entirely real quasienergy spectrum and pseudo-Hermitian dynamics. Conversely, if the particle hops on a finite linear chain with open boundary conditions, the energy spectrum is entirely real for a stationary gauge field but can become complex via multiple parametric resonances in an oscillating field. Our results highlight the very different physics of tight-binding lattices driven by either real or imaginary gauge fields, providing important novel insights into the dynamical behavior in the non-Hermitian case. The present analysis could be extended into several directions; for example, by considering mixed real and imaginary gauge fields as well as two-dimensional lattice geometries.

APPENDIX: MULTIPLE PARAMETRIC RESONANCES IN A LINEAR LATTICE WITH OPEN BOUNDARY CONDITIONS: SECULAR PERTURBATION THEORY

In this appendix we present a secular perturbation theory of Eq. (2), showing the appearance of multiple parametric resonances, leading to complex quasienergies, in the limit of a small gauge field $h(t) \to 0$. Without loss of generality, we assume that $h(t)$ is an ac field with zero mean; a nonvanishing dc value h_0 of the periodic function $h(t)$ can be eliminated by the gauge transformation $c_n(n) \to c_n(t) \exp(-h_0 n)$ and hence it does not affect the quasienergy spectrum of the Hamiltonian. For $|h(t)| \ll 1$, one can write $\exp[\pm h(t)] \simeq 1 \pm h(t)$ and

Eq. (2) takes the form

$$i\frac{d\mathbf{c}}{dt} = \mathcal{A}\mathbf{c} + h(t)(\mathcal{B}_1 - \mathcal{B}_2)\mathbf{c}, \qquad (A1)$$

where $\mathbf{c} \equiv (c_1, c_2, \ldots, c_N)^T$ is the vector of the site occupation amplitudes and the $N \times N$ matrices $\mathcal{A}$, $\mathcal{B}_1$, and $\mathcal{B}_2$ are defined by

$$\mathcal{A}_{n,m} = \kappa(\delta_{n,m-1} + \delta_{n,m-1}), \qquad (A2)$$

$$(\mathcal{B}_1)_{n,m} = \kappa\delta_{n,m-1}, \qquad (A3)$$

$$(\mathcal{B}_2)_{n,m} = \kappa\delta_{n,m+1}, \qquad (A4)$$

$$(\mathcal{B}_1 - \mathcal{B}_2)_{n,m} = \kappa(\delta_{n,m-1} - \delta_{n,m+1}) \qquad (A5)$$

$(n,m = 1,2,\ldots,N)$. Let us indicate by $\mathcal{T}$ and $\mathcal{E}$ the eigenvector matrix and corresponding diagonal eigenvalue matrix of $\mathcal{A}$, i.e., such that $\mathcal{A}\mathcal{T} = \mathcal{T}\mathcal{E}$. The explicit forms of $\mathcal{T}$ and $\mathcal{E}$ read

$$\mathcal{T}_{n,m} = \sqrt{\frac{2}{N+1}}\sin\left(\frac{nm\pi}{N+1}\right), \qquad (A6)$$

$$\mathcal{E}_{n,m} = E_n\delta_{n,m} = 2\kappa\cos\left(\frac{n\pi}{N+1}\right)\delta_{n,m}. \qquad (A7)$$

After setting $\mathbf{c}(t) = \mathcal{T}\mathbf{a}(t)$, i.e., in the basis that diagonalizes $\mathcal{A}$, Eq. (A1) can be cast in the form

$$i\frac{d\mathbf{a}}{dt} = \mathcal{E}\mathbf{a} + h(t)\mathcal{P}\mathbf{a}, \qquad (A8)$$

where we have set

$$\mathcal{P} \equiv \mathcal{T}^{-1}(\mathcal{B}_1 - \mathcal{B}_2)\mathcal{T}. \qquad (A9)$$

Taking into account that $\mathcal{T}^{-1} = \mathcal{T}$, after some cumbersome algebra one can derive the following expression of the elements of the time-independent perturbation matrix $\mathcal{P}$ entering in Eq. (A8):

$$\mathcal{P}_{n,m} = \kappa\frac{1 - (-1)^{n+m}}{N+1}\sin\left(\frac{m\pi}{N+1}\right)$$
$$\times\left[\cot g\frac{\pi(n+m)}{2(N+1)} + \cot g\frac{\pi(n-m)}{2(N+1)}\right]. \qquad (A10)$$

Note that $\mathcal{P}$ is an anti-Hermitian matrix, i.e., $\mathcal{P}_{n,m} = -\mathcal{P}_{m,n}^*$, and $\mathcal{P}_{n,m}$ vanishes when $|n + m|$ is an even number. In the absence of the oscillating gauge field $h = 0$, the dynamical system described by Eq. (A8) is neutrally stable because the energies E_n are real. The addition of the perturbation term on the right-hand side of Eq. (A8) can lead to secularly growing terms via typical parametric resonance phenomena, corresponding to complex quasienergies. To capture the onset of parametric resonances, we perform a rather standard secular perturbation analysis of Eq. (A8) by letting $h(t) \to \alpha h(t)$, where α is a smallness parameter that indicates the order of magnitude of the various terms entering in the asymptotic analysis (see, for instance, Refs. [31,33]). We look for a solution to Eq. (A8) as a power series in α:

$$\mathbf{a} = \mathbf{a}^{(0)} + \alpha\mathbf{a}^{(1)} + \alpha^2\mathbf{a}^{(2)} + \cdots, \qquad (A11)$$

and introduce multiple timescales

$$T_0 = t, \quad T_1 = \alpha t, \quad T_2 = \alpha^2 t, \ldots, \qquad (A12)$$

which are necessary to remove secular growing terms that would prevent the asymptotic expansion (A11) to be uniformly valid in time. The substitution of Eq. (A11) into Eq. (A8) and the use the derivative rule $(d/dt) = (d/dT_0) + \alpha(d/dT_2) + \alpha^2(d/dT_2) + \cdots$ yields a hierarchy of equations at successive orders in α. At lowest order $\sim\alpha^0$ one obtains $i(da_n^{(0)}/dT_0) = E_n a_n^{(0)}$, which yields

$$a_n^{(0)} = A_n(T_1, T_2, \ldots)\exp(-iE_nT_0), \qquad (A13)$$

where the amplitudes A_n are allowed to vary on the slow timescales $T_1, T_2, \ldots$. At order $\sim\alpha$ one obtains

$$\left(i\frac{d}{dT_0} - E_n\right)a_n^{(1)} = G_n^{(1)}(T_0), \qquad (A14)$$

where we have set

$$G_n^{(1)} \equiv -i\frac{\partial A_n}{\partial T_1}\exp(-iE_nT_0)$$
$$+ h(T_0)\sum_{m=1}^{N}\mathcal{P}_{n,m}A_m\exp(-iE_mT_0). \qquad (A15)$$

To avoid the appearance of secularly growing terms when solving Eq. (A14), the driving term $G_n^{(1)}$ defined by Eq. (A15) should not contain a term oscillating like $\sim\exp(-iE_nT_0)$. The solvability conditions thus yield the following coupled equations for the evolution of the amplitudes A_n on the slow timescale T_1:

$$i\frac{dA_n}{dT_1} = \sum_{m=1}^{N}\mathcal{R}_{n,m}\mathcal{A}_m, \qquad (A16)$$

where we have set

$$\mathcal{R}_{n,m} \equiv \mathcal{P}_{n,m}\langle h(t)\exp[i(E_n - E_m)t]\rangle \qquad (A17)$$

and the brackets $\langle\ldots\rangle$ on the right-hand side of Eq. (A17) denotes time average of the oscillating term. Since $h(t)$ is real and periodic with period $T = 2\pi/\omega$, the matrix element $\mathcal{R}_{n,m}$ does not vanish provided that the resonance condition

$$E_n - E_m \pm l\omega \simeq 0 \qquad (A18)$$

is satisfied for some integer l, with $l \neq 0$ [34]. This is the resonance condition given by Eq. (17) in the text. From Eqs. (A10) and (A17), it can be readily shown that the matrix $\mathcal{R}$ is anti-Hermitian, i.e., its eigenvalues are purely imaginary. Moreover, if λ is an eigenvalue of $\mathcal{R}$, then λ^* is an eigenvalue as well. Therefore, provided that some of the elements of the matrix $\mathcal{R}$ do not vanish, the solution to Eq. (A16) shows secularly growing terms on the timescale T_1, i.e., the quasienergies of the time-periodic system (A1) become complex with an imaginary part of order $\sim\alpha$. This explains the existence of multiple parametric resonance tongues found in the numerical computation of the quasienergies, shown in Fig. 3. As the number N of lattice sites increases, the number of resonance tongues, as determined by the resonance condition (A18), rapidly increases below the cutoff frequency 4κ.

It should be noted that, since $\mathcal{R}_{n,m}$ vanishes when $|n-m|$ is an even number, some of the resonance tongues predicted by Eq. (A18) can be missed. Let us discuss, for example, the simplest case of $N=3$ lattice sites. In this case the three eigenvalues E_l read

$$E_1 = \sqrt{2}\kappa, \quad E_2 = 0, \quad E_3 = -\sqrt{2}\kappa. \quad \text{(A19)}$$

Therefore, according to Eq. (A18) resonance tongues are expected to emanate from the two sets of frequencies

$$\omega_l^{(1)} = \frac{|E_3 - E_1|}{l} = \frac{2\sqrt{2}\kappa}{l}, \quad \text{(A20)}$$

$$\omega_l^{(2)} = \frac{|E_2 - E_1|}{l} = \frac{|E_3 - E_2|}{l} = \frac{\sqrt{2}\kappa}{l}, \quad \text{(A21)}$$

with $l = 1, 2, 3, \ldots$. However, since $\mathcal{P}_{13} = \mathcal{P}_{31} = 0$, the family of resonances $\omega_l^{(1)}$ is missed. Moreover, for a square-wave modulation like that considered in Fig. 3 only odd Fourier amplitudes of $h(t)$ do not vanish, i.e., for the family of resonances $\omega_l^{(2)}$ only those with an odd integer l should be considered. Therefore, the actual resonance tongues in a linear chain with $N=3$ sites emanate from the frequencies $\sqrt{2}\kappa$, $\sqrt{2}\kappa/3$, $\sqrt{2}\kappa/5, \ldots$, in agreement with the numerical results shown in Fig. 3(a).

---

[1] J. J. M. Verbaarschot, H. A. Weidenmuller, and M. R. Zirnbauer, Phys. Rep. **129**, 367 (1985); N. Moiseyev, *ibid.* **302**, 212 (1998); J. G. Muga, J. P. Palao, B. Navarro, and I. L. Egusquiza, *ibid.* **395**, 357 (2004); I. Rotter, J. Phys. A **42**, 153001 (2009).

[2] N. Moiseyev, *Non-Hermitian Quantum Mechanics* (Cambridge University Press, Cambridge, UK, 2011).

[3] C. M. Bender and S. Boettcher, Phys. Rev. Lett. **80**, 5243 (1998); C. M. Bender, Rep. Prog. Phys. **70**, 947 (2007); C. M. Bender, D. C. Brody, and H. F. Jones, Phys. Rev. Lett. **89**, 270401 (2002).

[4] C. Keller, M. K. Oberthaler, R. Abfalterer, S. Bernet, J. Schmiedmayer, and A. Zeilinger, Phys. Rev. Lett. **79**, 3327 (1997); M. V. Berry, J. Phys. A **31**, 3493 (1998); M. V. Berry and D. H. J. O'Dell, *ibid.* **31**, 2093 (1998); R. Stützle, M. C. Göbel, Th. Hörner, E. Kierig, I. Mourachko, M. K. Oberthaler, M. A. Efremov, M. V. Fedorov, V. P. Yakovlev, K. A. H. van Leeuwen, and W. P. Schleich, Phys. Rev. Lett. **95**, 110405 (2005); M. Kreibich, J. Main, H. Cartarius, and G. Wunner, Phys. Rev. A **90**, 033630 (2014).

[5] J. P. Bouchaud and A. Georges, Phys. Rep. **195**, 127 (1990); M. B. Isichenko, Rev. Mod. Phys. **64**, 961 (1992).

[6] N. Hatano and D. R. Nelson, Phys. Rev. Lett. **77**, 570 (1996); Phys. Rev. B **56**, 8651 (1997); **58**, 8384 (1998).

[7] D. R. Nelson and N. M. Shnerb, Phys. Rev. E **58**, 1383 (1998).

[8] A. Kostenbauder, Y. Sun, and A. E. Siegman, J. Opt. Soc. Am. A **14**, 1780 (1997); A. Ruschhaupt, F. Delgado, and J. G. Muga, J. Phys. A **38**, L171 (2005); R. El-Ganainy, K. G. Makris, D. N. Christodoulides, and Z. H. Musslimani, Opt. Lett. **32**, 2632 (2007); K. G. Makris, R. El-Ganainy, D. N. Christodoulides, and Z. H. Musslimani, Phys. Rev. Lett. **100**, 103904 (2008); S. Klaiman, U. Günther, and N. Moiseyev, *ibid.* **101**, 080402 (2008); S. Longhi, *ibid.* **103**, 123601 (2009).

[9] A. Guo, G. J. Salamo, D. Duchesne, R. Morandotti, M. Volatier-Ravat, V. Aimez, G. A. Siviloglou, and D. N. Christodoulides, Phys. Rev. Lett. **103**, 093902 (2009); C. E. Rüter, K. G. Makris, R. El-Ganainy, D. N. Christodoulides, M. Segev, and D. Kip, Nat. Phys. **6**, 192 (2010); S. Longhi, Phys. Rev. Lett. **105**, 013903 (2010).

[10] L. Feng, M. Ayache, J. Huang, Y. L. Xu, M. H. Lu, Y. F. Chen, Y. Fainman, and A. Scherer, Science **333**, 729 (2011); L. Feng, Y.-L. Xu, W. S. Fegadolli, M.-H. Lu, J. E. B. Oliveira, V. R. Almeida, Y.-F. Chen, and A. Scherer, Nat. Mater. **12**, 108 (2012).

[11] P. W. Brouwer, P. G. Silvestrov, and C. W. J. Beenakker, Phys. Rev. B **56**, R4333(R) (1997); P. G. Silvestrov, *ibid.* **58**, R10111(R) (1998); N. M. Shnerb and D. R. Nelson, Phys. Rev. Lett. **80**, 5172 (1998); I. Ya. Goldsheid and B. A. Khoruzhenko, *ibid.* **80**, 2897 (1998); I. V. Yurkevich and I. V. Lerner, *ibid.* **82**, 5080 (1999); J. Feinberg and A. Zee, Phys. Rev. E **59**, 6433 (1999); A. V. Kolesnikov and K. B. Efetov, Phys. Rev. Lett. **84**, 5600 (2000); J. Heinrichs, Phys. Rev. B **63**, 165108 (2001); F. Hebert, M. Schram, R. T. Scalettar, W. B. Chen, and Z. Bai, Eur. Phys. J. B **79**, 465 (2011).

[12] T. Fukui and N. Kawakami, Phys. Rev. B **58**, 16051 (1998); C. Mudry, B. D. Simons, and A. Altland, Phys. Rev. Lett. **80**, 4257 (1998); K. Takeda and I. Ichinose, J. Phys. Soc. Jpn. **70**, 3623 (2001); L. G. Molinari, J. Phys. A **42**, 265204 (2009).

[13] S. Longhi, D. Gatti, and G. Della Valle, Sci. Rep. **5**, 13376 (2015).

[14] S. Longhi, D. Gatti, and G. Della Valle, Phys. Rev. B **92**, 094204 (2015).

[15] S. Longhi, Phys. Rev. A **92**, 042116 (2015).

[16] W. H. Hu and Z. Song, Phys. Rev. A **84**, 052310 (2011); W. H. Hu, L. Jin, and Z. Song, Quantum Inf. Process. **12**, 3569 (2013).

[17] D. H. Dunlap and V. M. Kenkre, Phys. Rev. B **34**, 3625 (1986); M. Holthaus, Phys. Rev. Lett. **69**, 351 (1992); M. M. Dignam and C. M. de Sterke, *ibid.* **88**, 046806 (2002); S. Longhi and K. Staliunas, Opt. Commun. **281**, 4343 (2008).

[18] F. Grossmann, T. Dittrich, P. Jung, and P. Hänggi, Phys. Rev. Lett. **67**, 516 (1991); F. Grossmann and P. Hänggi, Europhys. Lett. **18**, 571 (1992); M. Grifoni and P. Hänggi, Phys. Rep. **304**, 229 (1998).

[19] K. W. Madison, M. C. Fischer, R. B. Diener, Q. Niu, and M. G. Raizen, Phys. Rev. Lett. **81**, 5093 (1998); H. Lignier, C. Sias, D. Ciampini, Y. Singh, A. Zenesini, O. Morsch, and E. Arimondo, *ibid.* **99**, 220403 (2007); E. Kierig, U. Schnorrberger, A. Schietinger, J. Tomkovic, and M. K. Oberthaler *ibid.* **100**, 190405 (2008); A. Eckardt, M. Holthaus, H. Lignier, A. Zenesini, D. Ciampini, O. Morsch, and E. Arimondo, Phys. Rev. A **79**, 013611 (2009); A. Zenesini, H. Lignier, D. Ciampini, O. Morsch, and E. Arimondo, Phys. Rev. Lett. **102**, 100403 (2009).

[20] S. Longhi, M. Marangoni, M. Lobino, R. Ramponi, P. Laporta, E. Cianci, and V. Foglietti, Phys. Rev. Lett. **96**, 243901 (2006); R. Iyer, J. S. Aitchison, J. Wan, M. M. Dignam, and C. M. de Sterke, Opt. Express **15**, 3212 (2007); G. Della Valle,

M. Ornigotti, E. Cianci, V. Foglietti, P. Laporta, and S. Longhi, Phys. Rev. Lett. **98**, 263601 (2007); A. Szameit, I. L. Garanovich, M. Heinrich, A. A. Sukhorukov, F. Dreisow, T. Pertsch, S. Nolte, A. Tünnermann, S. Longhi, and Y. S. Kivshar, *ibid.* **104**, 223903 (2010); S. Longhi, Phys. Rev. A **71**, 065801 (2005).

[21] See, for instance, M. Lewenstein, A. Sanpera, V. Ahunger, B. Damski, A. Sen, and U. Sen, Adv. Phys. **56**, 243 (2007); P. Hauke, O. Tieleman, A. Celi, C. Ölschläger, J. Simonet, J. Struck, M. Weinberg, P. Windpassinger, K. Sengstock, M. Lewenstein, and A. Eckardt, Phys. Rev. Lett. **109**, 145301 (2012); N. Goldman, G. Juzeliunas, P. Ohberg, and I. B. Spielman, Rep. Prog. Phys. **77**, 126401 (2014); L. Lu, J. D. Joannopoulos, and M. Soljacic, Nat. Photonics **8**, 821 (2014).

[22] G. Della Valle and S. Longhi, Phys. Rev. A **87**, 022119 (2013).

[23] X. Luo, J. Huang, H. Zhong, X. Qin, Q. Xie, Y. S. Kivshar, and C. Lee, Phys. Rev. Lett. **110**, 243902 (2013).

[24] J. D'Ambroise, B. A. Malomed, and P. G. Kevrekidis, Chaos **24**, 023136 (2014); A. A. Zyablovsky, E. S. Andrianov, and A. A. Pukhov, Sci. Rep. **6**, 29709 (2016).

[25] Y. N. Joglekar, R. Marathe, P. Durganandini, and R. K. Pathak, Phys. Rev. A **90**, 040101 (2014).

[26] J. Gong and Q.-H. Wang, Phys. Rev. A **91**, 042135 (2015).

[27] T. E. Lee and Y. N. Joglekar, Phys. Rev. A **92**, 042103 (2015).

[28] D. D. Scott and Y. N. Joglekar, Phys. Rev. A **85**, 062105 (2012).

[29] D. D. Scott and Y. N. Joglekar, J. Phys. A: Math. Theor. **45**, 444030 (2012).

[30] I. V. Barashenkov, L. Baker, and N. V. Alexeeva, Phys. Rev. A **87**, 033819 (2013).

[31] A. P. Seyranian and A. A. Mailybaev, *Multiparameter Stability Theory with Mechanical Applications*, Series on Stability, Vibration and Control of Systems, Series A (World Scientific, Singapore, 2003), Vol 13.

[32] I. Hoveijn and M. Ruijgrok, Z. Angew Math. Phys. **46**, 384 (1995); I. Bena and C. Van den Broeck, Europhys. Lett. **48**, 498 (1999); A. P. Markeyev, J. Appl. Math. Mech. (Engl. Transl.) **70**, 176 (2006); P. Danzl and J. Moehlis, Nonlinear Dyn. **59**, 661 (2010).

[33] J.-S. Chen and Y.-R. Lin, J. Vib. Acoust. **120**, 303 (1998); R. Lifshitz and M. C. Cross, Phys. Rev. B **67**, 134302 (2003); S. Longhi, *ibid.* **77**, 195326 (2008).

[34] For a sinusoidal modulation $h(t) = h_1 \sin(\omega t)$, only the first harmonic $l = 1$ should be taken in Eq. (A18), since higher-order Fourier harmonic amplitudes vanish for a sinusoidal modulation. This holds in first-order perturbation theory, i.e., up to the time scale T_1, which captures first-order resonance tongues. However, pushing the asymptotic analysis to higher orders, i.e., by considering the evolution of the amplitudes A_n at the longer time scales $T_2, T_3, \ldots$, higher harmonics of the modulation frequency ω appear even for a sinusoidal modulation. This is well known, for example, for the usual asymptotic theory of parametric resonance in the Mathieu equation. Hence Eq. (A18) with arbitrary l can be regarded as the general multiple parametric resonance condition.